PHYSICAL REVIEW B **89**, 081303(R) (2014)

Experimental observation of exciton splitting and relaxation dynamics from PbS quantum dots in a glass matrix

Fangyu Yue,[1,2,*] Jens W. Tomm,[1] and D. Kruschke[3]

[1]*Max-Born-Institut für Nichtlineare Optik und Kurzzeitspektroskopie, Max-Born-Straße 2A, 12489 Berlin, Germany*

[2]*Key Laboratory of Polar Materials and Devices, Ministry of Education, East China Normal University, 200241 Shanghai, Peoples's Republic of China*

[3]*Institut für Angewandte Photonik e.V., Rudower Chaussee 29/31, 12489 Berlin, Germany*

(Received 4 November 2013; revised manuscript received 27 December 2013; published 10 February 2014)

Multiple optical transitions from PbS quantum dots (QDs) in glass matrix are observed. Energy separations between them amount up to ∼200 meV. Instead of being due to a size distribution of QDs, they are found to be related to a splitting of the lowest exciton levels. Systematic analysis of the relaxation dynamics reveals the lifetimes of the split states ranging from sub-100-ns to ∼μs. Moreover, we observe excited and "intrinsic" states having a sub-100-ps and ∼ns lifetime, respectively. The behavior of the split structure can be modeled by a phonon-assisted relaxation mechanism. This investigation offers a conclusive interpretation for the wide distribution of experimentally observed nonequilibrium carrier lifetimes in PbS QDs.

DOI: 10.1103/PhysRevB.89.081303 PACS number(s): 81.07.Ta, 78.55.−m, 71.70.Gm, 78.47.da

Lead salt (e.g., PbS) quantum dots (QDs) have been widely investigated for applications in optoelectronic devices [1,2]. The QDs are either colloidal or embedded into a glass matrix. The latter provides substantial advantages in terms of long-term stability [3]. In order to evaluate and improve the properties of materials or devices, the QD size and its distribution as well as the excitonic lifetime are major issues, which should be accurately characterized, e.g., directly by optical methods including steady-state (SS) or transient absorption and photoluminescence (PL) spectroscopy at room temperature [4].

However, in rock salt PbS QDs the dimension of the excitonic manifold is theoretically 64 because both the valence-band maximum and the conduction-band minimum originate from the 8-fold (including spin) L valleys in the first Brillouin zone of bulk PbS. The degeneracy of these L valleys becomes lifted due to, e.g., intervalley coupling, interband coupling, and electron-hole Coulomb and exchange interaction [5]. Another mechanism potentially acting into this direction is external forces such as pressure as well as a special chemical surrounding, e.g., in a matrix. The split structure makes the optical transition in QDs complex and affects the characterization of QD features including the lowest excitonic transition energy (for simplicity called E_g) and subsequently the size and distribution of QDs as well as the nonequilibrium carrier recombination mechanism. In spite of the fact that asymmetric- or multi-PL (or absorption) peaks from these kinds of QDs have been observed even at room temperature, no direct reports involve these split states. Typically extrinsic assumptions are made including size distribution (e.g., multimodal QDs) [6], temperature/excitation-induced broadening [7], or defect states [8,9].

In this Rapid Communication, PbS QDs embedded in a borosilicate glass matrix are prepared and characterized by SS- or transient-PL spectroscopy at low excitation densities and temperatures. A three-transition structure from the QDs is observed with an energy separation up to 200 meV, in dependence of growth conditions including annealing. The intrinsic mechanism for this three-transition structure that seems to be sensitive to the host matrix, e.g., with borosilicate but not with silicate-glass matrix, is attributed to a splitting of the lowest excitons in a single-size QD system, instead of assumptions of size distribution and excited excitonic states. The results on relaxation dynamics show that the lifetime of these split states ranges from sub-100-ns to ∼μs. In addition, we observe excited and "intrinsic" states having a lifetime of sub-100-ps and ∼ns, respectively. Moreover, we also find that the split structure can be described by a phonon-assisted exciton relaxation model.

Samples were grown with the compositions SiO_2: 51.5, Al_2O_3: 7.5, B_2O_3: 15.3, Na_2O: 11.4, PbS: 1.6, PbO: 0.9, ZnO: 0.8, ZnS: 0.8, CaO: 4.8, K_2O: 5.4 (mass %), and followed by a two-stage annealing process (the first stage for crystallization and the second stage for tuning the QD size) [10,11]. Sample plates were polished with thicknesses from ∼50 μm to 3 mm. PL was measured by a Fourier transform infrared spectrometer equipped with 77-K-cooled Ge and HgCdTe detectors. Excitation was provided by cw or pulsed 1.06-μm- or 442-nm-emitting lasers. Besides the standard reflectance-PL geometry (R-PL), "transmission"-PL (T-PL) was implemented by exciting the sample on one side while collecting signal from the other side. PL decays were recorded for two pulse conditions: (i) at a low repetition rate of 10 kHz with 1.06 μm excitation (detection was made by an InGaAs photodiode connected with a GHz oscilloscope), and (ii) at a high repetition rate of 80 MHz from a Tsunami Ti:sapphire laser with 100 fs pulse duration at 800 nm; here detection was provided by a Hamamatsu synchroscan streak camera with an S1 photocathode (temporal resolution better than 10 ps). Note that sufficiently low excitation densities (cw ∼ sub W/cm^{-2} and pulse ∼ μJ/cm^{-2}) ensured to detect the intrinsic transition mechanism. Temperatures were adjusted from 5 K to 300 K.

Figure 1(a) shows the PL spectrum of a sample at 5 K with cw excitation (sub W/cm^{-2}). There are three PL peaks. Gaussian fits locate the three peaks marked by A, B, and C at ∼1.53 μm, 1.39 μm, and 1.24 μm, respectively. The energy differences between them are ∼83 meV ($E_B - E_A$)

*yue@mbi-berlin.de

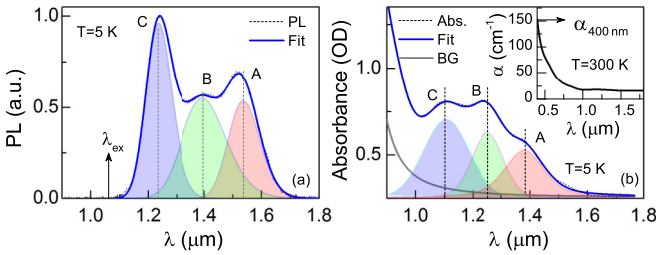

FIG. 1. (Color online) PL (a) and absorption (b) spectra of a sample at 5 K together with the fit results. λ_{ex} in (a) is the excitation wavelength. Curve BG in (b) represents a broad fit background. The inset in (b) gives the absorption spectrum at 300 K that covers the wavelength ranges down to 400 nm.

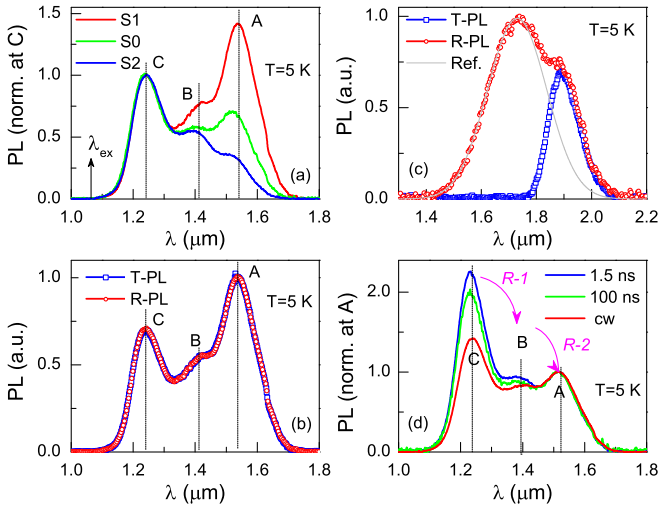

FIG. 2. (Color online) (a) PL spectra (normalized to peak C) at 5 K of samples annealed at different conditions (S_1: 560 °C/22 h + 640 °C/85 min; S_0: 560 °C/22 h + 640 °C/75 min; S_2: 560 °C/22 h + 630 °C/90 min). (b) R-PL and T-PL spectra of S_1 at 5 K. (c) R-PL and T-PL spectra at 5 K of a multimodal (or size-graded) sample as a reference. (d) PL spectra (normalized to peak A) of S_0 at 5 K for cw (<1 W/cm^2) and pulsed excitation modes (~100 ns pulse width at ~2 μJ/cm^2; ~1.5 ns pulse width at ~5 μJ/cm^2). The arrows represent the assumed carrier/exciton relaxation process between states.

and 196 meV ($E_C - E_A$). Note that increasing excitation density or temperature smears the three-line structure towards a broad asymmetric single-spectral shape. Figure 1(b) gives the absorption spectrum at 5 K. Again a multitransition structure is observed. Gaussian-fits locate three main transitions marked also by A, B, and C at ~1.38 μm, 1.24 μm, and 1.10 μm, respectively. It should be pointed out that no pronounced PL and absorption peaks are observed in reference samples prepared by replacing PbS with PbO and ZnS with ZnO, verifying that the three-structure definitely originates from the PbS QDs.

A three-transition structure makes the QD system complex. Excitation density dependent measurements show the three peaks to behave in a similar way including their peak energy, full width at half maximum (FWHM), and intensity. Even thermal effects observed at the highest density appear in the same way for all three features. This indicates that the three peaks are not defect-related emissions. However, their evolution with temperature reveals evident differences. Only the energy and FWHM of peak A show monotonic increase with temperature while those of peaks B and C evolve obviously nonmonotonically (see Supplemental Material [12]). A reproduction on the results of peak A by employing the Fan function [13] and a semiempirical phonon-broadening expression (for FWHM) [14] yields key parameters including the temperature coefficient 347 μeV/K, the average phonon temperature 198 ± 17 K, and the longitude optical (LO) phonon coupling coefficient 50 ± 4 meV with the LO phonon energy of ~14 meV as well as the phonon-coupling number of 1.9 [15]. These values are well consistent with theoretical and experimental reports [9,16,17]. This suggests that the lowest energy peak A can be tentatively assigned to the excitonic ground state transition of the QDs (which would correspond to the biggest QDs, if peaks B and C were assumed to be created by a size distribution). The average radius of the QDs can be then calculated to ~3.35 nm according to a hyperbolic-band model [18]. The volume fraction f of these QDs in glass matrix is deduced to ~0.07% by referring to the absorption coefficient of 400 nm at 300 K [see the inset in Fig. 1(b)] [11]. The average distance between QDs is then estimated to $\bar{d} \approx 70$ nm assuming a cubic arrangement of QDs in the glass matrix. Such a low f value (as well as the big $\bar{d}$ value) rules out any energy transfer mechanisms [19,20] such as carrier/exciton relaxation between closest QDs (called electronic energy transfer/EET) or the cascade excitation process between QDs with different sizes (i.e., Förster resonance energy transfer/FRET); also see Supplemental Material [12].

Figure 2(a) shows PL spectra of samples annealed at different conditions. It is well-known that annealing conditions (temperature and/or time) influence QD size and distribution [10]. However, the three-PL lines are independent of any annealing. More important, the lowest peak A shows a redshift and becomes stronger as the second-stage annealing temperature or time increases, while the highest peak C together with the middle B does not show any shift. This implies that attributing peak A to E_g of QDs (corresponding to intrinsic QD sizes) is reasonable. But peaks B and C are not related to other QD sizes, which will be discussed below, because the slight redshift (or intensity increase) of peak A means the growing (or concentration increase) of QDs by increasing annealing temperature/time.

Figure 2(b) displays PL spectra of a sample (thickness ~3 mm) taken in T-PL and R-PL geometries at 5 K. It is interesting to note that the T-PL shows exactly the same three-peak structure as the R-PL. T-PL is an effective method that reveals reabsorption processes, e.g., if a size distribution of QDs exists [21]. Figure 2(c) shows this for a reference sample with a multimodal size distribution prepared by a graded-annealing process (thickness also ~3 mm). From Fig. 2(c) we can see that two (Gaussian) fit curves can be displayed in the standard R-PL geometry, but only the low-energy peak appears in the spectrum obtained in T-PL. Similar results were also observed in previous size-in-order samples [10]. Obviously, all high-energy emission from the smaller dots gets reabsorbed. The data presented in Fig. 2(b), however, illustrate that the three-transition structure cannot be caused by any QD size distribution. Using 442 nm excitation (sub W/cm^2), besides

the three peaks being at the same spectral position as for 1.06 μm excitation, an additional shoulder peak at ~1.1 μm appears even in T-PL geometry. This further confirms our line of arguments. Therefore, it can be inferred that the three peaks A–C are not related to three kinds of QD sizes but from different states within a single QD, and the additional peak at ~1.1 μm (~320 meV higher than the lowest peak A) for excitation at 442 nm is likely to be from a high-energy state in the single-size QD system, e.g., an excited state.

Figure 2(d) shows PL spectra at 5 K under cw and pulsed excitations. It is evident that the relative intensity of the high-energy peaks B and C can be increased by pulsed excitation as compared to cw excitation. A similar result was also reported in Ref. [22], which was taken as experimental evidence that this kind of multistructure in PL spectra is not derived from defect states. However, further comparison between the two pulsed results (~1.5 ns and ~100 ns) discloses that the highest peak C together with the middle B can be enhanced by the shorter pulse duration of 1.5 ns. This suggests that the three transitions own different lifetimes, i.e., $\tau_C < \tau_B < \tau_A$, as depicted in the figure with the relaxation process of *R-1* from C to B and *R-2* from B to A.

Figure 3(a) further shows typical PL decays after excitation by ~1.5 ns pulses (10 kHz repetition rate) at 5 K and 300 K. Note that single exciton generation per QD is ensured (at least 2 orders of magnitude of photons per pulse lower than that of QD numbers in the laser beam volume, defined as $N_{ex} < 0.01$). The curves show a multiexponential behavior. A three-exponential

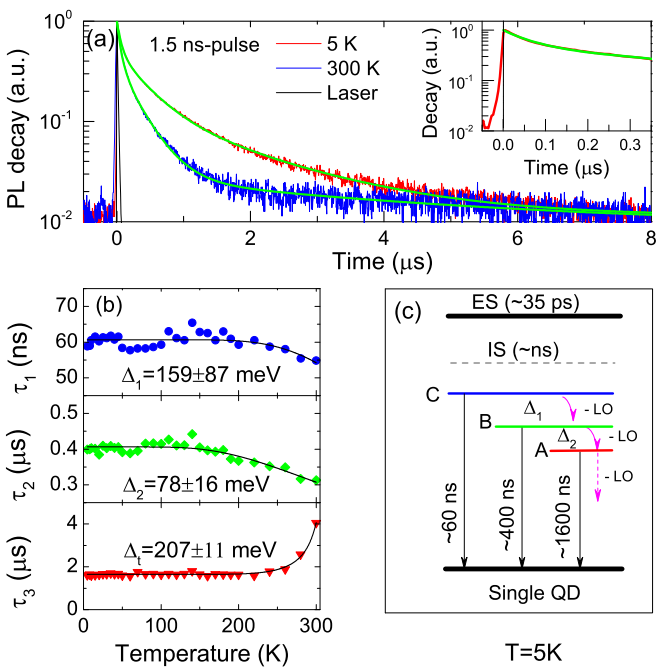

FIG. 3. (Color online) (a) Decay curves at 5 K and 300 K after 1.5 ns pulse excitation and (b) the temperature dependence of lifetimes. The inset in (a) amplifies the part at the beginning of the exciton decay. The solid lines in (a) and (b) are fit results. (c) Schematic of the excitonic fine structure including the excited state (ES), the "intrinsic" state (IS), and the split states (A–C) in a single QD at 5 K. As the temperature increases, the LO phonon assisted relaxation among these states will be enhanced.

decay function fits best. It yields three lifetimes of $\tau_1 \sim 60$ ns, $\tau_2 \sim 400$ ns, and $\tau_3 \sim 1.6$ μs at 5 K (and 55 ns, 310 ns, and 4.1 μs, respectively, at 300 K). Combined with the result in Fig. 2(d) and the corresponding description in the text (e.g., $\tau_C < \tau_B < \tau_A$) as well as the previous attribution of peak A to the intrinsic E_g of QDs, τ_3 points to a μs lifetime typically for a ground-state-related lifetime in such QDs (i.e., peak A in Fig. 1); see reports on spontaneous emission lifetimes of PbS QDs [9,23,24].

Figure 3(b) summarizes the temperature dependencies of the lifetimes τ_i ($i = 1, 2, 3$). It should be emphasized that τ_i remain almost constant at first but then evolve with different behaviors at temperatures over ~180 K, where τ_1 and τ_2 decrease while the slowest τ_3 increases. This represents a temperature-induced transfer of carriers/excitons from the state related to τ_1 or τ_2 to the state of τ_3 (increasing the exciton concentration of the τ_3 state) [25]. This is again in full agreement with a relaxation mechanism as proposed in Fig. 2(d).

Taking into account the temperature range above ~180 K pointing to the activation of LO phonons (~14 meV) and the strong LO-phonon coupling effect in the system (as discussed before), it can be deduced that the LO-phonon coupling plays an important role for the temperature dependence of the relaxation processes. Therefore, a rate function describing the relaxation/activation process between states is employed to model the dynamics of the carrier transfer [26], $r = 1/\tau = r_0 + r_{nr}/[\exp(\Delta/k_BT) - 1]$, where k_B is the Boltzmann constant, Δ is the energy difference between two states, r_0 is a zero-temperature relaxation rate, and r_{nr} is a rate constant related to phonon coupling. Fit operation on τ_i ($i = 1,2,3$) gives $\Delta_1 = 159 \pm 87$ meV with $r_0 = 0.02$ ns^{-1}, $\Delta_2 = 78 \pm 16$ meV with $r_0 = 2.46$ μs^{-1}, and $\Delta_t = 207 \pm 11$ meV with $r_0 = 0.61$ μs^{-1}, respectively. Here, Δ_t can be understood as a state with the energy of $(\Delta_1 + \Delta_2)$ that can be activated from the τ_3 state with an "activation" rate of r_{nr}. From the fit we can see that Δ_t is close to the value of $(\Delta_1 + \Delta_2)$. Back to the foregoing results [see, e.g., Fig. 2(d)], we can also find these fit results based on the temperature dependence of lifetime to be in fair agreement with the results earlier obtained by optical spectroscopy (i.e., $E_C - E_B = 121$ meV, $E_B - E_A = 81$ meV, and subsequently $E_C - E_A = 202$ meV). Therefore, a relaxation scheme for levels A–C can be proposed; see Fig. 3(c). This demonstrates that the highest state (peak C) being located at ~121 meV above peak B gives radiative recombination with a lifetime of ~60 ns (at 5 K). Carriers relax to peak B due to the LO-phonon coupling, from where excitons decay with a lifetime of ~400 ns, and further relax to the lowest peak A, which lies at ~81 meV below peak B. There the lifetime amounts to ~1.6 μs.

In order to disclose potentially even faster relaxation process related to excited states in this system, 100 fs pulse excitation with a much higher repetition rate of 80 MHz (as compared to the foregoing 10 kHz) is employed to excite samples. Figure 4(a) shows transient PL data taken at 5 K ($N_{ex} < 0.01$). Besides a slow component at ~1.05 μm (IS) there is a fast component within ~100 ps (ES; energetically almost continuous toward the cutoff set by an edge filter at 895 nm). It is worth mentioning that the carrier/exciton accumulation of the slow component is relatively small

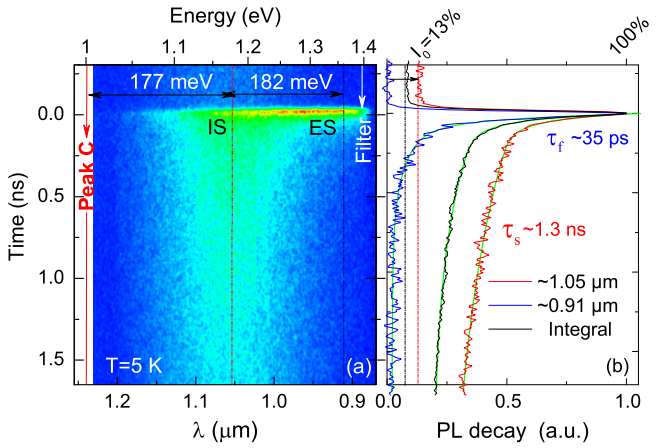

FIG. 4. (Color online) (a) Transient PL image at pulsed 800 nm excitation with a repetition rate of 80 MHz (5 K). The cutoff at ∼1.4 eV is caused by an edge filter. "Peak C" denotes the spectral position of peak C in Figs. 1–3. (b) Decay curves extracted from (a) at the wavelengths of ∼1.05 μm (red) and ∼0.91 μm (blue). Black is the spectral integration result. The two-exponential decay function fit (green) gives a fast and slow decay time of ∼35 ps (blue) and ∼1.3 ns (red), respectively.

[∼13%, also see Fig. 4(b)], in spite of the much shorter pulse circle (12.5 ns) compared to the "regular" spontaneous emission of ∼μs lifetime in PbS QDs (e.g., peak A in Fig. 1).

Figure 4(b) gives the decay curves at ∼1.05 μm and ∼0.91 μm as well as the spectrally integrated result. From this figure we can see that from the high-energy ES state (∼0.91 μm) to the main IS state (∼1.05 μm), the surviving tail gradually increases, and consequently the background due to the accumulation of carriers also increases (up to $I_0 = 13\%$). A two-exponential decay function fit indicates that the "fast" lifetime is ∼35 ps, while the "slow" one is ∼1.3 ns. Note that the "slow" lifetime here is substantially smaller than that of the well-known regular spontaneous emission (e.g., ∼μs of peak A in Fig. 1) and even "faster" by an order of magnitude than those being related to peaks B and C. Attention should be paid also to the peak position at ∼1.05 μm (∼1.181 eV), which is evidently blueshifted compared to the peaks in Fig. 1. This holds even for the highest-energy peak C (∼177 meV blueshift); also see Supplemental Material [12]. This demonstrates that the main component centered at ∼1.05 μm with a ∼ns lifetime should not be associated with the regular spontaneous emission in PbS QDs that has a ∼μs lifetime, but corresponds to another state. Keeping in mind the high repetition rate of 80 MHz, we can infer that this blueshifted transition is due to the excitation-induced "band-filling" effect, which fills in all states of peaks A–C (due to the long lifetime from sub-100-ns to μs) until to this high-energy state (with ∼ns lifetime). This phenomenon is also consistent with our previous work [27], where we called it the "intrinsic" state that corresponds to the first exciton absorption energy of the QDs. Back to the findings obtained using the 442 nm excitation, which caused a PL shoulder at ∼1.1 μm, it is likely that the additional peak is related to this intrinsic state with a ∼ns lifetime. At this point, the fast component with the broad energy distribution (up to 182 meV) can be attributed to the higher energy states, e.g., excited states, by referring to the large energy difference with peaks A–C (e.g., ∼359 meV from peak C) [28] and the similar lifetime to reports for excited states in lead salt QDs [29,30]. This has been added to the scheme of the dynamics shown in Fig. 3(c), where the excited states have a ∼35 ps lifetime to relax to the "IS" state which has a ∼ns lifetime.

Now we come to the nature of the three peaks A–C in our PbS QDs. Note that this triple structure occurs in a single-QD-size system because the hypothesis on a three-modal size distribution of QDs has been excluded by combining (i) the large distance between QDs (∼70 nm) and the similar results of T-PL and R-PL spectra; (ii) the fundamentally different temperature dependencies of peak energy and FWHM of the three peaks, where only the lowest peak A showing a monotonous evolution; (iii) the by about 2 orders of magnitude different lifetimes of the three transitions; and (iv) the fact that experimentally, it is highly unlikely that different syntheses made by different groups would lead to very similar multimodal size distributions [31]. An assignment of peaks B and C to excited states can be eliminated by taking into account (i) that well-established theories [32,33] predict an energy separation of at least 350 meV between the excited states from the ground-state excitonic energy in PbS QDs and the separation strikingly increases as the QDs become smaller, which is much larger than our values of $(E_B - E_A)$ and $(E_C - E_A)$; and (ii) that experiments [29,30] including the present results reveal the lifetime of ps∼sub-100-ps for excited states in lead salt QDs, which is much shorter than those of peaks B and C (sub-100-ns to sub-μs). In view of the 64-degeneracy of the lowest-energy exciton due to the 8 (half) L valleys in the first Brillouin zone, one can assume that the observed complex triple-transition structure is related to the split of the lowest exciton level. A theoretical investigation has reported an intervalley splitting energy up to ∼100 meV in PbSe QDs [5], but unfortunately no results for PbS QDs are available.

We should point out that the three-transition structure is observed here for PbS QDs in borosilicate glass matrix (also co-doped with K_2O), while in reference samples prepared in silicate glass matrix no multioptical transition structure has been observed so far. This finding underlines the impact of host matrices to the intervalley splitting of PbS QDs. Moreover, this points to "external forces" such as pressure or the chemical surrounding as additional mechanisms, which are likely to increase the intervalley splitting beyond the above quoted theoretical numbers. In addition, it should be mentioned that it is difficult to directly observe the separated three-transitions by optical spectroscopy at high temperatures or excitation densities because of the thermally induced broadening or excitation-induced "band-filling" effects; also see Fig. 4. There the emission being centered at ∼1.05 μm is almost close to the absorption position of peak C [see Fig. 1(b)], suggesting that at frequently used experimental conditions the split states are filled in different ratios. This makes PL spectra degenerate and subsequently the lifetime represents complex temperature or excitation dependencies and varies within the range from the well-established ∼μs to sub-100-ns [4,5,27,29,34].

In summary, a triple-peak structure of the lowest excitons is experimentally observed in PbS QDs in borosilicate glass matrix with a rather narrow QD size distribution.

Relaxation dynamics reveals the lifetimes of the split structure components ranging from sub-100-ns to $\sim\mu$s together with "intrinsic" and excited states having a lifetime of ~ns and sub-100-ps, respectively. The split structure can be modeled by a phonon-assisted recombination rate function, which is consistent with the energy separations determined from optical spectra. These results provide additional implementations: (i) T-PL can be employed as an option to analyze the QD size distribution, if compared to the standard R-PL geometry; (ii) the intervalley splitting in PbS QDs can be enhanced by ~200 meV by the choice of the host (which impacts to the dots as additional "external force"); (iii) low temperatures rather than frequently used room temperature are vital to evaluate the QD sizes and their distributions. Moreover, our investigation offers a conclusive interpretation of the rather wide distribution of lifetimes reported in the literature for spontaneous emission from lead salt QDs.

This work is supported by the FRFCU (78260024), the NSFC (61376103), and the BMWi-Germany (MF090215).

[1] E. U. Rafailov, M. A. Cataluna, and W. Sibbett, Nat. Photon. **1**, 395 (2007).
[2] V. I. Klimov, Science **290**, 314 (2000).
[3] K. Wundke, J. Auxier, A. Schulzgen, N. Peyghambarian, and N. F. Borrelli, Appl. Phys. Lett. **75**, 3060 (1999).
[4] H. Du, C. L. Chen, R. Krishnan, T. D. Krauss, J. M. Harbold, F. W. Wise, M. G. Thomas, and J. Silcox, Nano Lett. **2**, 1321 (2002).
[5] J. M. An, A. Franceschetti, and A. Zunger, Nano Lett. **7**, 2129 (2007).
[6] E. V. Ushakova, A. P. Litvin, P. S. Parfenov, A. V. Fedorov, M. Artemyev, A. V. Prudnikau, I. D. Rukhlenko, and A. V. Baranov, ACS Nano **6**, 8913 (2012).
[7] S. Rudin, T. L. Reinecke, and B. Segall, Phys. Rev. B **42**, 11218 (1990).
[8] D. G. Kim, T. Kuwabara, and M. Nakayama, J. Lumin. **119**, 214 (2006).
[9] M. S. Gaponenko, A. A. Lutich, N. A. Tolstik, A. A. Onushchenko, A. M. Malyarevich, E. P. Petrov, and K. V. Yumashev, Phys. Rev. B **82**, 125320 (2010).
[10] F. Y. Yue, J. W. Tomm, D. Kruschke, P. Glas, K. A. Bzheumikhov, and Z. C. Margushev, Opt. Express **21**, 2287 (2013).
[11] I. Moreels, D. Kruschke, P. Glas, and J. W. Tomm, Opt. Mater. Express **2**, 496 (2012).
[12] See Supplemental Material at http://link.aps.org/supplemental/10.1103/PhysRevB.89.081303 for additional experimental results or descriptions.
[13] H. Fan, Phys. Rev. **82**, 900 (1951).
[14] C. Kammerer, C. Voisin, G. Cassabois, C. Delalande, P. Roussignol, F. Klopf, J. P. Reithmaier, A. Forchel, and J. M. Gerard, Phys. Rev. B **66**, 041306(R) (2002).
[15] A factor, $1/\exp(n\hbar\omega/k_BT)$ (n is the phonon number), is introduced into expressions by considering their saturation behavior at high temperatures due to phonon coupling.
[16] B. Ullrich, X. Y. Xiao, and G. J. Brown, J. Appl. Phys. **108**, 013525 (2010).
[17] A. D. Yoffe, Adv. Phys. **50**, 1 (2001).
[18] K. K. Nanda, F. E. Kruis, and H. Fissan, Nano Lett. **1**, 605 (2001).
[19] W. Lü, I. Kamiya, M. Ichida, and H. Ando, Appl. Phys. Lett. **95**, 083102 (2009).
[20] I. L. Medintz, H. T. Uyeda, E. R. Goldman, and H. Mattoussi, Nat. Mater. **4**, 435 (2005).
[21] B. Ullrich, R. Schroeder, and H. Sakai, Semicond. Sci. Technol. **16**, L89 (2001).
[22] J. M. Harbold and F. W. Wise, Phys. Rev. B **76**, 125304 (2007).
[23] R. Espiau de Lamaestre, H. Bernas, D. Pacifici, G. Franzo, and F. Priolo, Appl. Phys. Lett. **88**, 181115 (2006).
[24] F. Y. Yue, J. W. Tomm, D. Kruschke, and P. Glas, Laser Photon. Rev. **7**, L1 (2013).
[25] P. Andreakou, M. Brossard, C. Li, M. Bernechea, G. Konstantatos, and P. G. Lagoudakis, J. Phys. Chem. C **117**, 1887 (2013).
[26] O. Labeau, P. Tamarat, and B. Lounis, Phys. Rev. Lett. **90**, 257404 (2003).
[27] F. Y. Yue, J. W. Tomm, and D. Kruschke, Phys. Rev. B **87**, 195314 (2013).
[28] J. Yang, B. R. Hyun, A. J. Basile, and F. W. Wise, ACS Nano **6**, 8120 (2012).
[29] B. L. Wehrenberg, C. J. Wang, and P. Guyot-Sionnest, J. Phys. Chem. B **106**, 10634 (2002).
[30] J. M. An, M. Califano, A. Franceschetti, and A. Zunger, J. Chem. Phys. **128**, 164720 (2008).
[31] D. Grodzinska, W. H. Evers, R. Dorland, J. van Rijssel, M. A. van Huis, A. Meijerink, C. D. Donega, and D. Vanmaekelbergh, Small **7**, 3493 (2011).
[32] I. Kang and F. W. Wise, J. Opt. Soc. Am. B **14**, 1632 (1997).
[33] B. Diaconescu, L. A. Padilha, P. Nagpal, B. S. Swartzentruber, and V. I. Klimov, Phys. Rev. Lett. **110**, 127406 (2013).
[34] P. S. Parfenov, A. P. Litvin, A. V. Baranov, E. V. Ushakova, A. V. Fedorov, A. V. Prudnikov, and M. V. Artemyev, Opt. Spectrosc. **112**, 868 (2012).